Electronic Supplementary Material (ESI) for Lab on a Chip.

Supplementary Information

Deciphering potential vascularization factors of on-chip co-cultured hiPSC-derived cerebral organoids.

Maneesha Shaji[1], Atsushi Tamada[2], Kazuya Fujimoto[1], Keiko Muguruma[2]*, Stanislav L. Karsten[1]*, Ryuji Yokokawa[1]*

[1]Department of Micro Engineering, Graduate School of Engineering, Kyoto University, Kyoto daigaku Katsura, Nishikyo-ku, Kyoto – 615-8540, Japan.

[2]Department of iPS Cell Applied Medicine, Kansai Medical University, 2-5-1 Shin-machi, Hirakata City, Osaka – 573-1010, Japan.

Corresponding authors: Keiko Muguruma, Stanislav L. Karsten, Ryuji Yokokawa[1]

Email: karsten.stanislav.3i@kyoto-u.ac.jp, muguruke@hirakata.kmu.ac.jp, and yokokawa.ryuji.8c@kyoto-u.ac.jp

This PDF file includes:

Figures S1 to S9
Tables S2, S3
Supplementary text data S1, S2
SI References

Other supplementary materials for this manuscript include the following:

Table S1

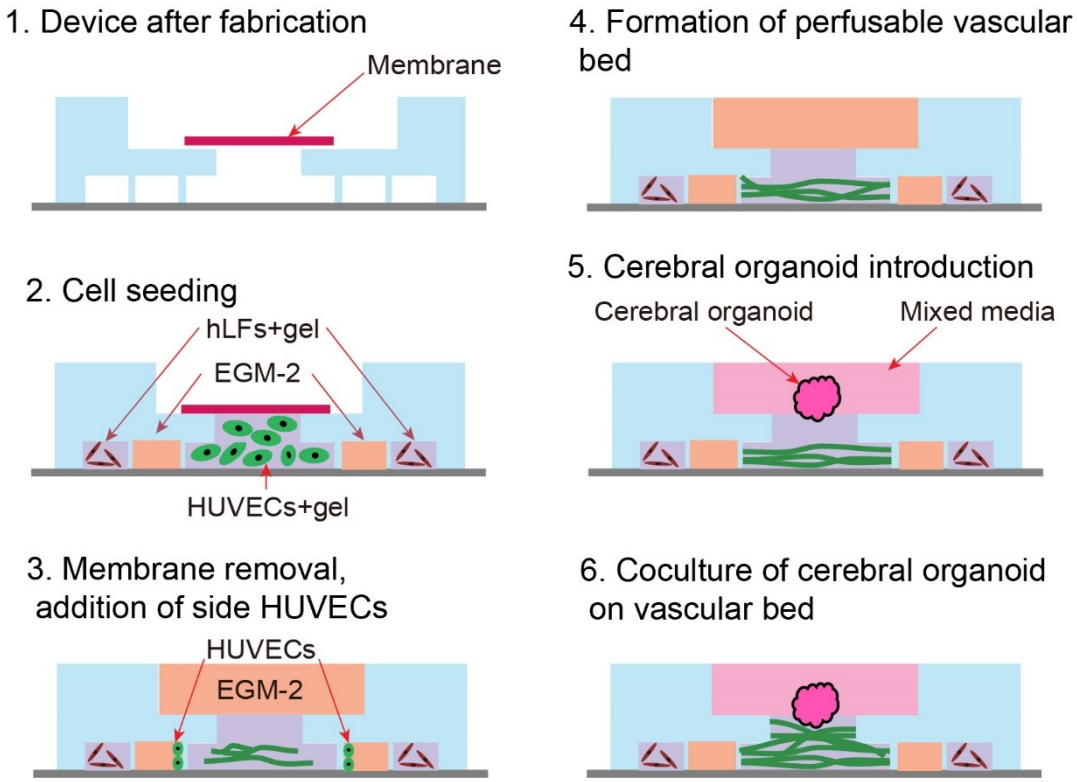

Fig. S1: Schematics showing the preparation of on-chip co-culture system.

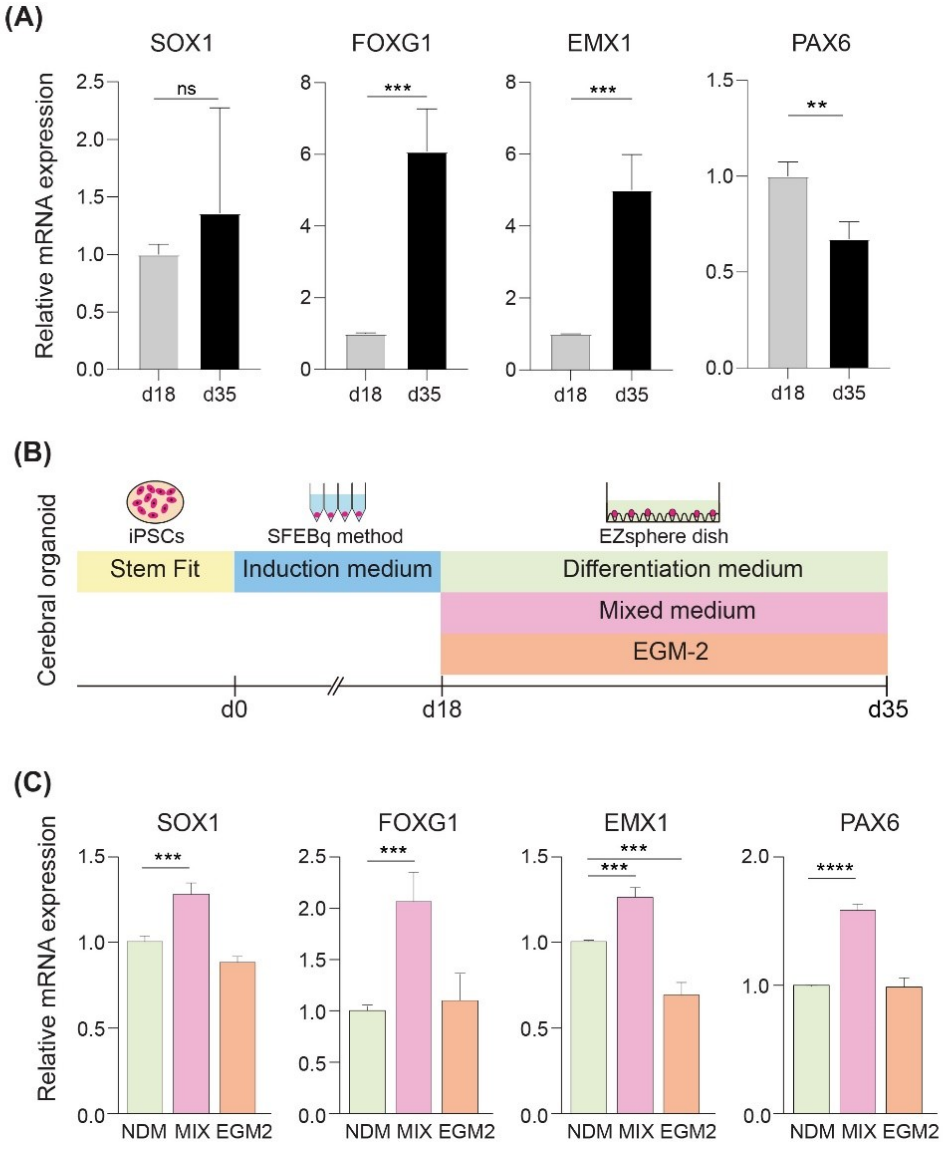

Fig. S2: Specificity of hiPSCs induction and evaluation of mixed culture media. (A) Relative gene expression of *SOX1*, *FOXG1*, *EMX1* and *PAX6* at organoid day 18 and day 35, n = 3. Two-tailed unpaired t-test was used for statistical significance. **(B)** The protocol for media optimization for co-culture experiment. **(C)** The relative gene expression of *SOX1*, *FOXG1*, *EMX1* and *PAX6* for day 35 organoids cultured in neural differentiation medium (NDM), endothelial growth medium 2 (EGM2) and mixed medium (MIX) from day 18 to day 35 on dish, n = 3. Dunnett's multiple comparison test (one-way ANOVA) with control as NDM, was used for statistical significance and only statistically significant values are shown. ** denotes $p < 0.01$, *** denotes $p < 0.001$, **** denotes $p < 0.0001$ and "ns" denotes not significant ($p > 0.05$).

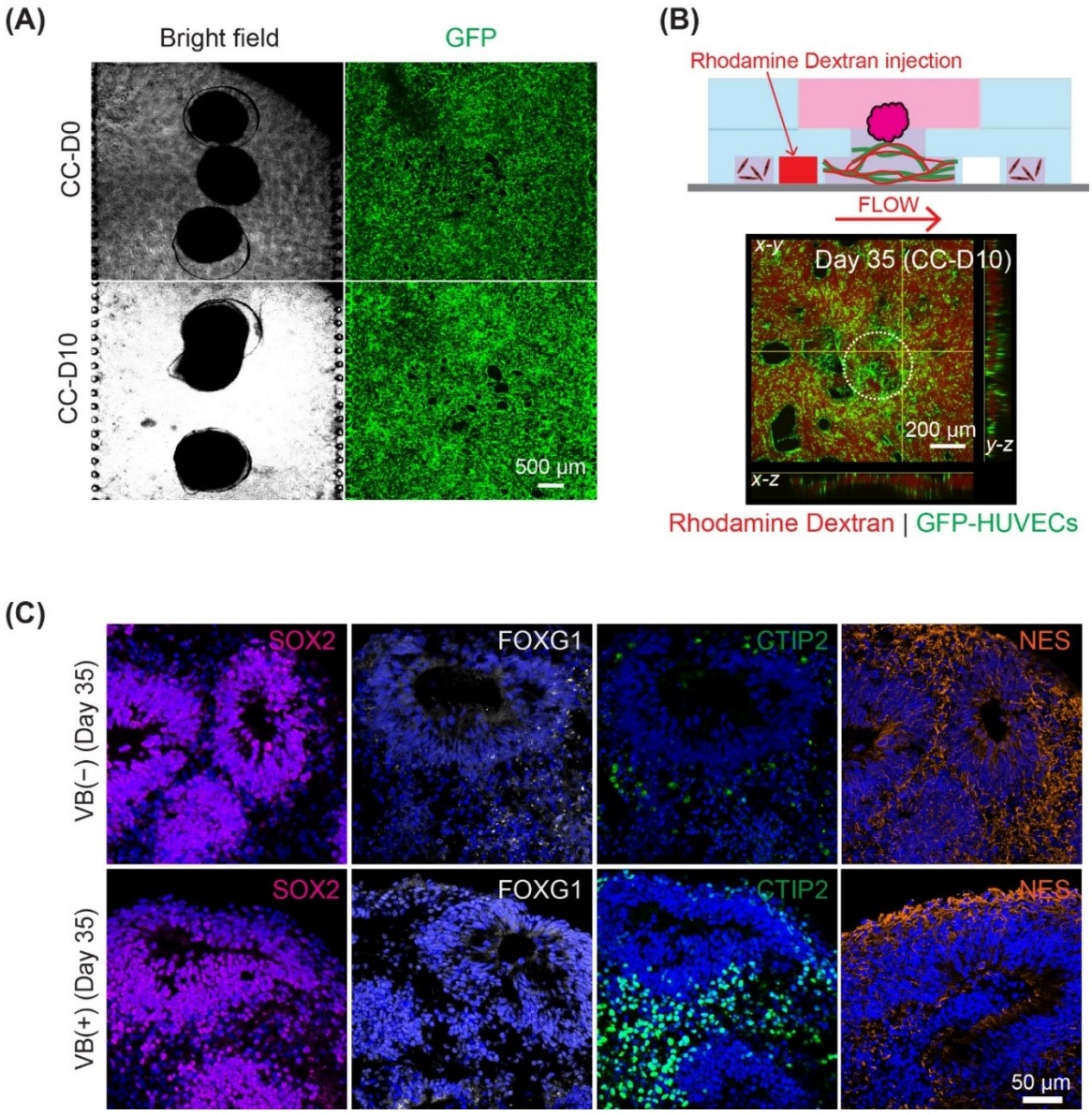

Fig. S3: On-chip co-culture of organoids. (A) Bright field (BF) and green fluorescent (GFP) images showing organoids and vasculature, respectively, at day 25 and day 35. **(B)** Confocal image showing the perfusability of vascular bed (VB) (shown in green) at day 35 is shown by flowing fluorescent rhodamine dextran (shown in red). White dotted circle shows the location of organoid. **(C)** Immunoassays of organoids cultured with and without VB at day 35. Nucleus is stained by DAPI (blue), progenitors by SOX2 (magenta), forebrain-specific marker by FOXG1 (white), differentiated neurons by CTIP2 (green) and neuroepithelial cells by NES (orange).

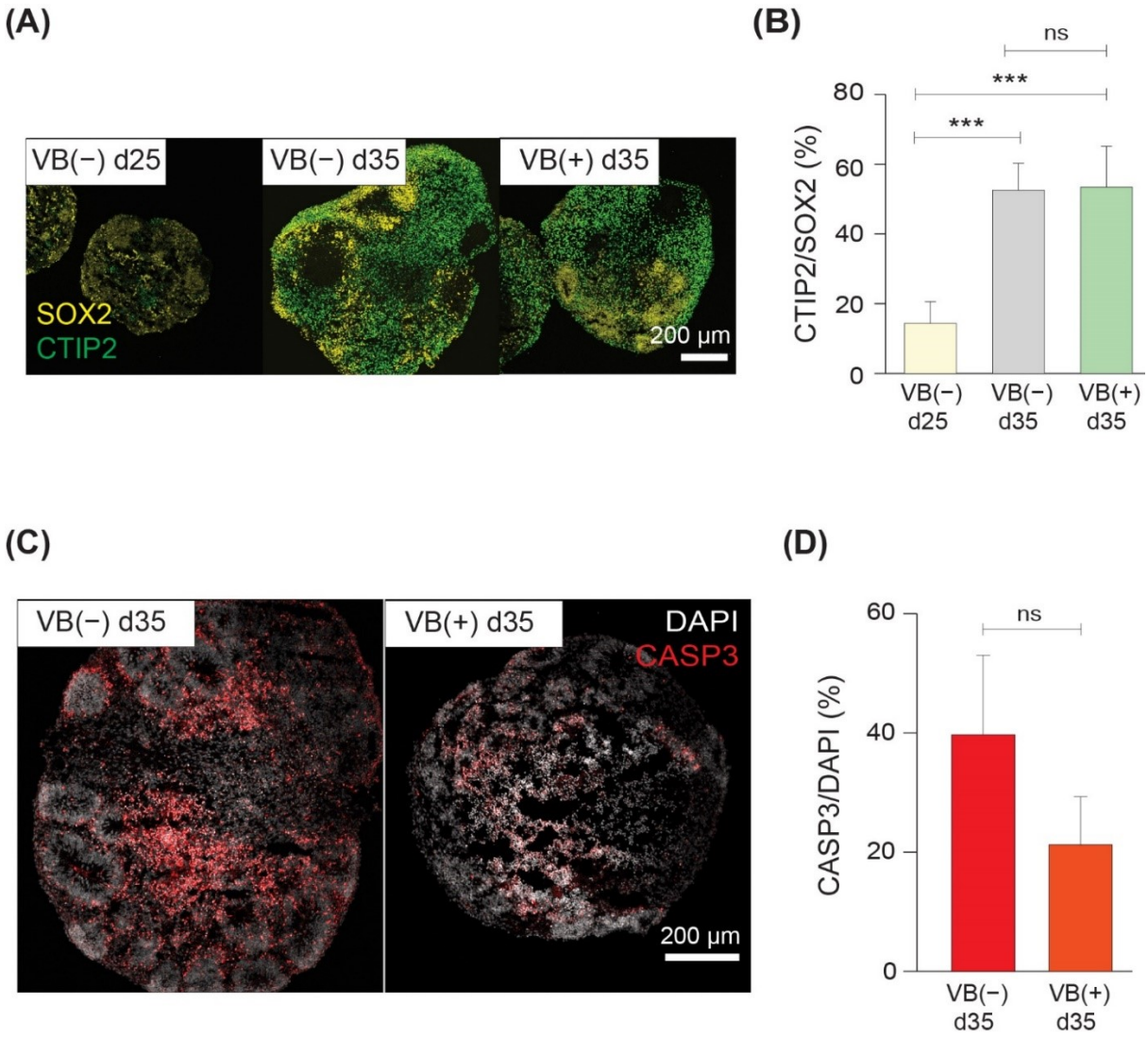

Fig. S4: Effect of vascular bed on organoid. (A) Immunostained images showing CTIP2 and SOX2 expressions of organoids at days 25 and 35 grown with and without vascular bed. **(B)** The percentage of expression of neuronal marker, CTIP2 relative to progenitor marker, SOX2 at day 25 and day 35 with and without vascular bed, n = 4. Tukey's multiple comparisons test (One-way ANOVA) was used for statistical significance test. **(C)** Immunostaining for apoptotic marker, CASP3 at day 35 for COs cultured with and without vascular bed. **(D)** The percentage of CASP3 expression relative to total number of cells (stained by DAPI) for organoids grown with and without vascular bed, n = 3. Two-tailed unpaired t-test was used for significance test. * denotes $p < 0.05$, *** denotes $p < 0.001$ and ns denotes not significant ($p > 0.05$).

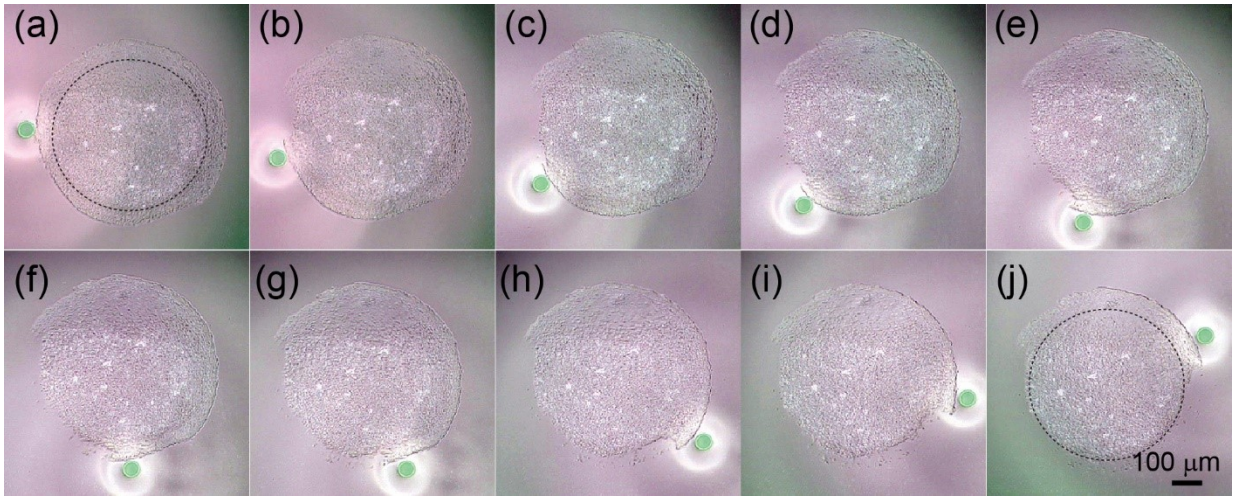

Fig. S5: Representative microdissections of outer cortical layer of organoids using UnipicK+ (NeuroInDx, Inc., CA, USA). The dotted circle shown in figure separates the outer cortical layer from necrotic core. The green bright circle is the tip of the capillary used to collect the cells with UnipicK+.

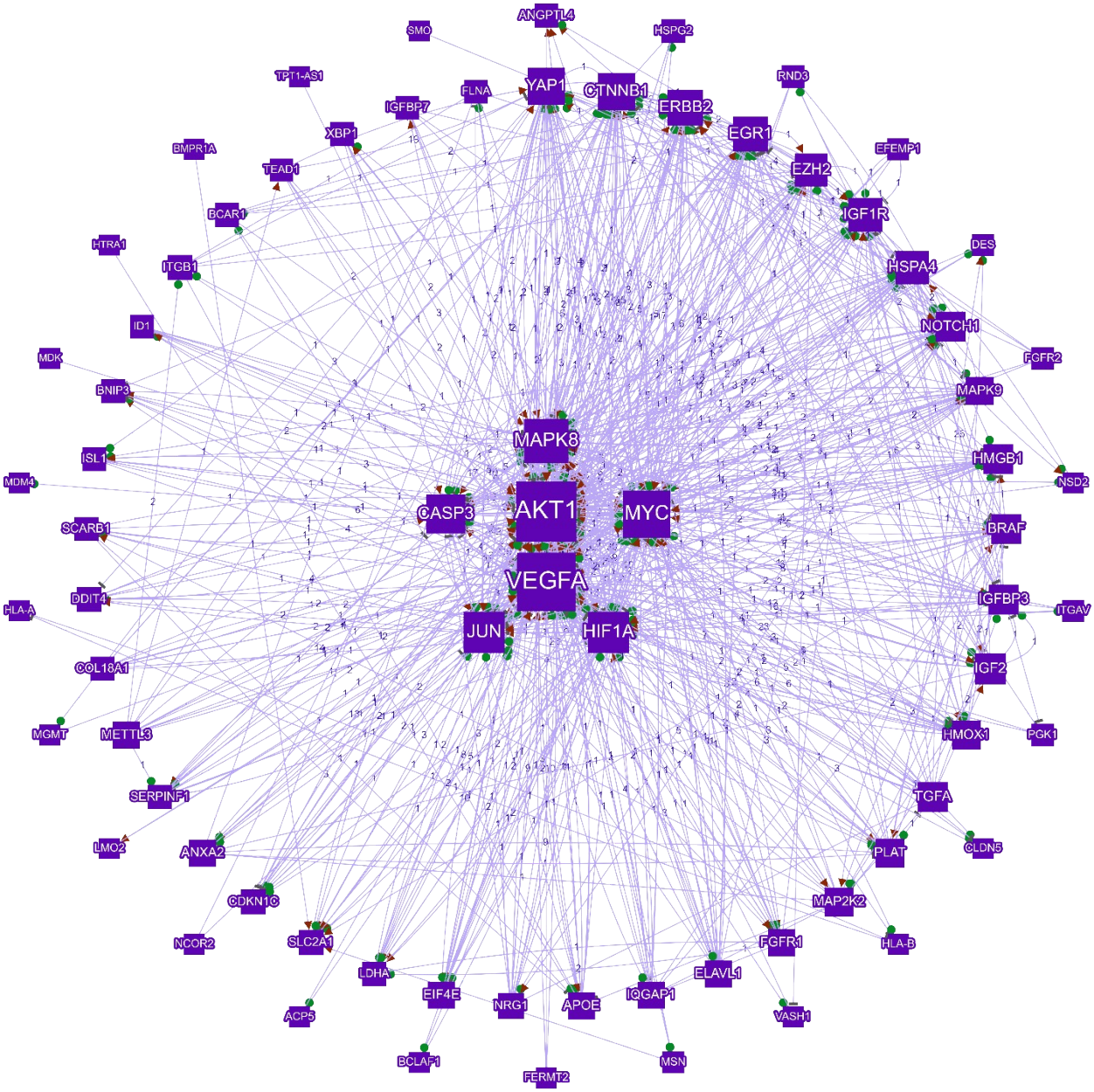

Fig. S6: Enriched cluster of angio- and vasculogenesis related genes identified with DAVID functional annotation enrichment analysis.

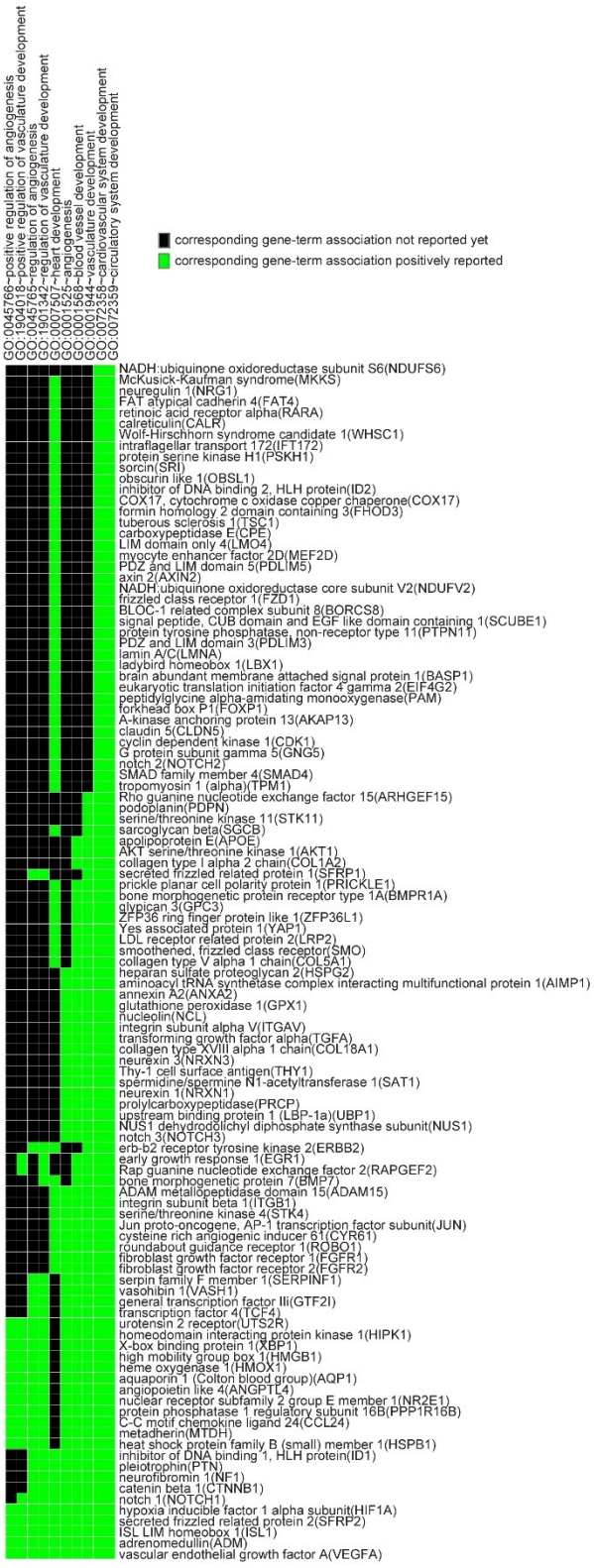

Fig. S7: GenCLiP literature-based network of angiogenesis related genes.

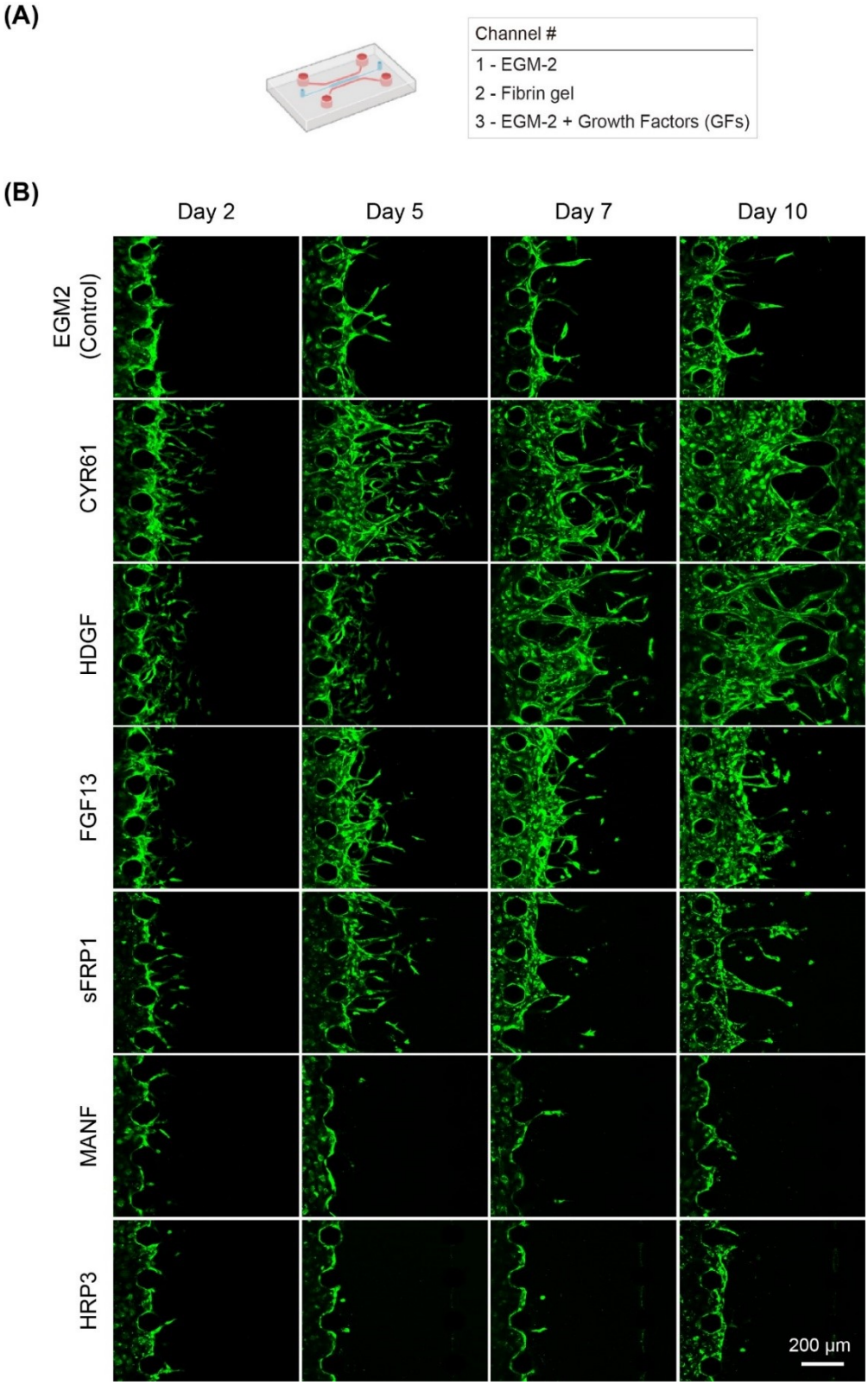

Fig. S8: On-chip sprouting assay for identified growth factors. (A) The schematic of the 3-channel microfluidic device used for evaluation of angiogenesis and vasculogenesis. **(B)** Time lapse images showing the angiogenic sprouts (shown in green) at days 2, 5, 7 and 10 induced by CYR61, HDGF, FGF13, sFRP1, MANF, and HRP3 using the angiogenesis assay. The images for control, CYR61 and HDGF at day 2 and 10 were reused from the fig. 5B.

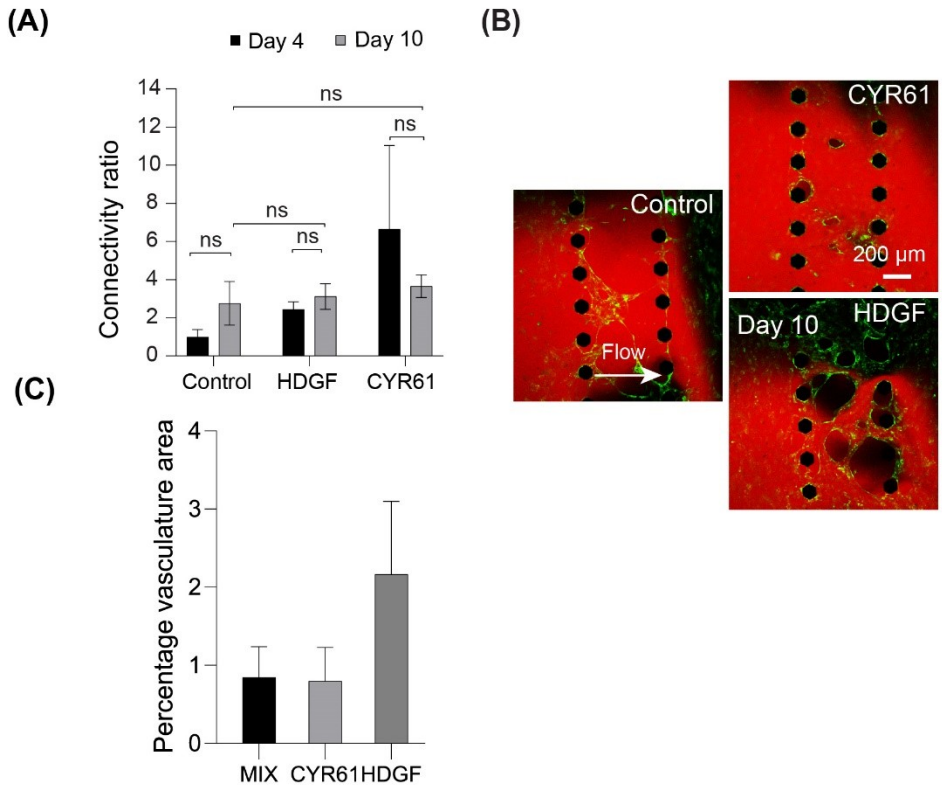

Fig. S9: On-chip vasculogenesis assay shows the vascular network formed by identified growth factors. (A) Connectivity ratio of the networks formed in the presence of CYR61 and HDGFs, n= 4. Tukey's multiple comparison test (two-way ANOVA) was used for significance test, ns denotes no significance $p > 0.05$. **(B)** Perfusability of the vascular networks (green) at day 10, by flowing rhodamine dextran (red). White arrow shows the flow direction of the rhodamine dextran. **(C)** Percentage area covered by vasculature inside CO grown in the presence of CYR61, HDGF and mixed media at day 10 of co-culture. The area was calculated using CO cryosections.

Table S1. (separate file)

Angiogenesis-related genes with altered expression at days 31 and 35 of CO-VB co-culture identified with DAVID functional annotation clustering and GeneClip (GC) literature search. Growth factors are labeled with yellow.

Table S2.

Enriched biological processes identified with DAVID functional categorization tool. EASE score = 0.05.

GO Biological Process Term	Fold Enrichment	p value	Main Process
GO:0001525~angiogenesis	1.63	0.0002	vascular syst.
GO:0001666~response to hypoxia	1.56	0.0005	
GO:0048545~response to steroid hormone	1.53	0.0003	
GO:0030855~epithelial cell differentiation	1.53	0.0000	
GO:0010721~negative regulation of cell development	1.52	0.0005	
GO:0010769~regulation of cell morphogenesis involved in differentiation	1.47	0.0013	
GO:0007186~G-protein coupled receptor signaling pathway	1.47	0.0002	
GO:0051961~negative regulation of nervous system development	1.46	0.0029	CNS
GO:0007015~actin filament organization	1.43	0.0048	
GO:0001568~blood vessel development	1.42	0.0014	vascular syst.
GO:0001944~vasculature development	1.42	0.0009	vascular syst.
GO:0022604~regulation of cell morphogenesis	1.42	0.0002	
GO:0050801~ion homeostasis	1.41	0.0010	
GO:1901652~response to peptide	1.41	0.0028	
GO:0032870~cellular response to hormone stimulus	1.40	0.0004	
GO:2001233~regulation of apoptotic signaling pathway	1.40	0.0024	apoptosis

GO:1902532~negative regulation of intracellular signal transduction	1.39	0.0013	
GO:1903829~positive regulation of cellular protein localization	1.38	0.0039	
GO:0006873~cellular ion homeostasis	1.37	0.0069	
GO:0043434~response to peptide hormone	1.36	0.0089	
GO:0097190~apoptotic signaling pathway	1.34	0.0010	apoptosis
GO:0007507~heart development	1.34	0.0059	vascular syst.
GO:0071363~cellular response to growth factor stimulus	1.32	0.0027	
GO:0071407~cellular response to organic cyclic compound	1.32	0.0068	
GO:0030334~regulation of cell migration	1.32	0.0051	
GO:1903827~regulation of cellular protein localization	1.31	0.0021	
GO:0043408~regulation of MAPK cascade	1.31	0.0052	
GO:0072359~circulatory system development	1.30	0.0011	vascular syst.
GO:0072358~cardiovascular system development	1.30	0.0011	vascular syst.
GO:0045664~regulation of neuron differentiation	1.30	0.0044	CNS

Table S3.

Primary and secondary antibodies used in the study.

Primary antibodies

Name	Host	Manufacturer	Cat. No.	Ratio used
CASP3	Rabbit	Cell Signaling	9661S	1:500
CD31	Mouse	BD Biosciences	555444	1:300
CD31 (Alexa Fluor 647 conj.)	Mouse	BioLegend	303111	1:300
CTIP2	Rat	Abcam	ab18465	1:1000
FOXG1	Rabbit	Abcam	ab18259	1:1000
NES	Mouse	Atlas Antibodies	AMAb90556	1:1000
SOX2	Goat	R&D systems	AF2018	1:400

Secondary antibodies

Name	Host	Anti-	Manufacturer	Cat. No.	Ratio used
Alexa Fluor 488	Donkey	Mouse	Thermo Fisher	A21202	1:1000
Alexa Fluor 488	Donkey	Rat	Thermo Fisher	A21208	1:1000
Cy3 555	Donkey	Mouse	Jackson	715-165-151	1:1000
Alexa Fluor 568	Donkey	Goat	Thermo Fisher	A11057	1:1000
Alexa Fluor 568	Donkey	Rabbit	Thermo Fisher	A10042	1:1000
Rhodamine Red-X	Donkey	Chicken	Jackson	703-295-155	1:1000
Alexa Fluor 647	Donkey	Goat	Jackson	705-605-147	1:500
Alexa Fluor 647	Donkey	Sheep	Thermo Fisher	A21448	1:1000
Alexa Fluor 647	Donkey	Mouse	Thermo Fisher	A31571	1:1000

Supplementary Text Data S1.

Regulation of VEGF regulators and targets agrees with the initiation of angiogenic process at day 31 followed by its inhibition by day 35 of co-culture.

VEGF activating factors included AKT serine/threonine kinase 1 (1) (↑d31), early growth response 1 transcription factor, EGR1 (2) (↑d31, ↓d35), Erb-b2 receptor tyrosine kinase 2 (3) (ERBP2;↑d31), fibroblast growth factor receptor 1, FGFR1 (4) (↑d31), heme oxygenase 1 (5) (HMOX1; ↑d31, ↑d35), insulin-like growth factor 2 (6) (IGF2; ↑d31), NOTCH2 (7–9) (↑d31), perlecan (10) (PRCAN, ↑d31), TPT1 antisense RNA (11) (TPT1-AS1; ↑d31), X-Box Binding Protein 1 (12) (XBP1; ↑d31), Yes associated protein 1, YAP1 (13) (↑d31). Silencing of filamin A (FLNA; ↑d31, ↓d35) reduces VEGF expression (14). Its elevated and dropped expression levels at days 31 and 35 respectively are in the agreement with increased expression of VEGFA at day 31 (Fig. 4).

Expression of VEGFA (↑d31) did not show the same elevation at a later time point (d35) that coincides with the significantly reduced levels of multiple VEGF and HIF1A activators including beta-catenin (15,16) (CNNB1; ↓d35), B-Raf proto-oncogene serine/threonine kinase (17) (BRAF, ↓d35), EGF-containing fibulin-like extracellular matrix protein 1 (18) (EFEMP1; ↓d35), enhancer of zeste homolog 2 (19) (EZH2; ↓d35), eukaryotic translation initiation factor 4E-like 1 (20) (EIF4E; ↓d35), EGR12 (↑d31, ↓d35), ELAV Like RNA Binding Protein 1 (21) (ELAVL1; ↓d35), FLNA (14) (↑d31, ↓d35), heat shock 70kDa protein 4 (22) (HSPA4; ↓d35), high mobility group protein 1 (23) (HMGB1; ↓d35), insulin-like growth factor 1 receptor (24) (IGF1R; ↓d35), c-Jun proto-oncogene (25) (JUN; ↓d35), methyltransferase like 3 (26) (METTL3; ↓d35), mitogen-Activated Protein Kinase 8 (27) (MAPK8; ↓d35), and NOTCH1 (28) (↓d35) (Fig. 4).

The expression of VEGFA (↑d31) is directly induced by hypoxia-inducible factor 1-alpha (HIF1A; ↓d35) at the transcriptional level under hypoxia (29,30). Four identified pro-angiogenic activators of HIF1A (↓d35) expression were significantly downregulated after one week of coculture (Fig. 4). This included BCL2-associated transcription factor 1 (31) (BCLAF1; ↓d35), E3 ubiquitin-protein ligase SIAH2 (32,33) (↓d35), filamin A (34) (FLNA; ↑d31; ~↓d35), and histone deacetylase 1 (35–37) (HDAC1; ↑d31-↓d35) (Fig. 4).

Interestingly, Filamin A (↑d31; ~↓d35) is an actin binding protein that links actin filaments to membrane glycoproteins. Filamin A is involved in remodeling the cytoskeleton to regulate cell shape

and migration. According to one report, this protein is a liaison between neural progenitor cells and vasculature, and its loss of function increases VEGFA production (38). Another report claimed that Filamin A physically interacts with HIF1a (↓d35) and promotes angiogenesis (34), therefore decrease of Filamin A expression should inhibit hypoxia induced angiogenesis that is in agreement with our data.

Several VEGF inhibitors including apolipoprotein E (39) (APOE, ↑d31), collagen, type XVIII, alpha 1 (40), COL18A1 (↑d31), insulin-like growth factor binding protein-3 (41) (IGBP3; ↑d31), and pigment epithelium-derived factor (42,43) (PEDF or SERPINF1, ↑d31), and vasohibin 1 (44,45) (VASH1; ↑d31) demonstrated elevated expression at day 31, which may contribute to the decrease of VEGFA expression by day 35 (Table S2).

Multiple direct targets of VEGF were identified in this study. Breast cancer anti-estrogen resistance protein 1 (BCAR1 or CAS1; ↑d31, ~↓d35) is a Src family kinase member activated by VEGF that induces angiogenic sprouting (39,46). ISL LIM homeobox transcription factor 1 (ISL1; ↓d31, ↓d35) promotes postnatal angiogenesis acting on endothelial cells and increasing VEGF production (47–50). ISL1 is regulated via VEGF and its suppression reduces retinal angiogenesis in vivo (51). Tumour necrosis factor receptor superfamily, member 25 (TNFRSF25, ↓d35) is a member of the TNF-receptor superfamily that mediates apoptosis and induces angiogenesis via VEGFA (52,53). Other VEGF co-regulated factors downregulated in d35 include insulin-like growth factor 1 receptor (54) (IGF1R; ↓d35). Other pro-angiogenic targets of VEGFA included annexin 2 (55,56) (ANXA2; ↑d31), inhibitor of DNA binding 1 (57) (ID1; ↑d31, ↓d35), insulin like growth factor binding protein 7, IGFBP7 (58,59) (↑d31), and LIM domain only 2 (60) (LMO2; ↑d31).

Several identified genes were both VEGFA targets and regulators representing either positive or negative feedback loops. For example, AKT1 (61) (↑d31) and YAP1 (↑d31) activate VEGFA (62) (↑d31) expression via HIF1A (↓d35) and both are in the positive feedback loop being activated by VEGF to ensure proper angiogenic response. Silencing of AKT in HUVECs significantly inhibits VEGF induced capillary-like tube formation (63). Other positive feedback loops included VEGF activators EGR1 (64) (↑d31, ↓d35), EZH2 (65) (↓d35), FGF2 (66) (↑d31), JUN (67) (↓d35), IGF2 (68) (↑d31) and NOTCH1 (69) (↓d35) (Fig. 4).

Supplementary Text Data S2.

Other pro-angiogenic factors and pathways are regulated in accordance with observed CO's angiogenic response.

Mutations in Lamin A (LMNA; ↑d31) result in dilated cardiomyopathy characterized by impaired angiogenesis and nitric oxide (NO) production (70). L-lactate dehydrogenase A chain (LDHA; ↑d31) catalyses the conversion of L-lactate and NAD to pyruvate and NADH in the anaerobic glycolysis. Because glycolysis is one of the major sources of adenosine 5'-triphosphate (ATP) required for extensive endothelial cell outgrowth from existing vascular network during angiogenesis, inhibition of key glycolytic enzymes including LDHA directly affects tip cell differentiation and sprouting angiogenesis (71,72). Moreover, direct release of LDHA from damaged neurons triggers and its inhibition suppresses angiogenesis CNS angiogenesis in vivo (73). Inhibition of serine/threonine protein kinase 26 (STK26 or MST4; ↑d31) promotes apoptosis and silences angiogenesis in retinoblastoma mice (74). Inhibitors of angiogenesis programmed cell death 5 (PDCD5; ↓d35) facilitates p53-dependent apoptosis (75). Loss of PDCD5 in endothelial cells increases microvessel sprouting in vitro (76), while its overexpression reduces angiogenesis of osteosarcoma cells via TGF-β1/Smad signaling pathway (77).

References.

1. Jiang, B.-H. & Liu, L.-Z. AKT Signaling in Regulating Angiogenesis. Current Cancer Drug Targets vol. 8 19–26 (2008).

2. Shimoyamada, H. et al. Early Growth Response-1 Induces and Enhances Vascular Endothelial Growth Factor-A Expression in Lung Cancer Cells. Am. J. Pathol. 177, 70–83 (2010).

3. Finkenzeller, G., Weindel, K., Zimmermann, W., Westin, G. & Marmé, D. Activated Neu/ErbB-2 Induces Expression of the Vascular Endothelial Growth Factor Gene by Functional Activation of the Transcription Factor Sp 1. Angiogenesis 7, 59–68 (2004).

4. Golfmann, K. et al. Synergistic anti-angiogenic treatment effects by dual FGFR1 and VEGFR1 inhibition in FGFR1-amplified breast cancer. Oncogene 37, 5682–5693 (2018).

5. Birrane, G., Li, H., Yang, S., Tachado D., S. & Seng, S. Cigarette smoke induces nuclear translocation of heme oxygenase 1 (HO-1) in prostate cancer cells: Nuclear HO-1 promotes vascular endothelial growth factor secretion. Int J Oncol 42, 1919–1928 (2013).

6. Pollak, M. Insulin and insulin-like growth factor signalling in neoplasia. Nat. Rev. Cancer 8, 915–928 (2008).

7. Gridley, T. Notch signaling in vascular development and physiology. Development 134, 2709–2718 (2007).

8. Gasperowicz, M. & Otto, F. The Notch Signalling Pathway in the Development of the Mouse Placenta. Placenta 29, 651–659 (2008).

9. Akil, A. et al. Notch Signaling in Vascular Endothelial Cells, Angiogenesis, and Tumor Progression: An Update and Prospective . Frontiers in Cell and Developmental Biology vol. 9 (2021).

10. Zoeller, J. J., Whitelock, J. M. & Iozzo, R. V. Perlecan regulates developmental angiogenesis by modulating the VEGF-VEGFR2 axis. Matrix Biol. 28, 284–291 (2009).

11. Zhang, Y. et al. Long non-coding RNA TPT1-AS1 promotes angiogenesis and metastasis of colorectal cancer through TPT1-AS1/NF90/VEGFA signaling pathway. Aging (Albany. NY). 12, 6191–6205 (2020).

12. Duan, Q. et al. Deregulation of XBP1 expression contributes to myocardial vascular endothelial growth factor-A expression and angiogenesis during cardiac hypertrophy in vivo. Aging Cell 15, 625–633 (2016).

13. Hooglugt, A., van der Stoel, M. M., Boon, R. A. & Huveneers, S. Endothelial YAP/TAZ Signaling in Angiogenesis and Tumor Vasculature . Frontiers in Oncology vol. 10 (2021).

14. Vitali, E. et al. FLNA is implicated in pulmonary neuroendocrine tumors aggressiveness and progression. Oncotarget 8, 77330–77340 (2017).

15. Easwaran, V. et al. β-Catenin Regulates Vascular Endothelial Growth Factor Expression in Colon Cancer. Cancer Res. 63, 3145–3153 (2003).

16. Kim, S., Xu, X., Hecht, A. & Boyer, T. G. Mediator Is a Transducer of Wnt/ß-Catenin Signaling. J. Biol. Chem. 281, 14066–14075 (2006).

17. Husain, A., Hu, N., Sadow, P. M. & Nucera, C. Expression of angiogenic switch, cachexia and inflammation factors at the crossroad in undifferentiated thyroid carcinoma with BRAFV600E. Cancer Lett. 380, 577–585 (2016).

18. Dou, C.-Y. et al. EFEMP1 inhibits migration of hepatocellular carcinoma by regulating MMP2 and MMP9 via ERK1/2 activity. Oncol Rep 35, 3489–3495 (2016).

19. Nakagawa, S. et al. Enhancer of zeste homolog 2 (EZH2) regulates tumor angiogenesis and predicts recurrence and prognosis of intrahepatic cholangiocarcinoma. HPB 20, 939–948 (2018).

20. Smith, M. R. & Costa, G. RNA-binding proteins and translation control in angiogenesis. FEBS J. n/a, (2021).

21. Osera, C. et al. Induction of VEGFA mRNA translation by CoCl2 mediated by HuR. RNA Biol. 12, 1121–1130 (2015).

22. Kawabata, T. et al. HSP70 Inhibitors Reduce The Osteoblast Migration By Epidermal Growth Factor. Current Molecular Medicine vol. 18 486–495 (2018).

23. Yang, S., Xu, L., Yang, T. & Wang, F. High-mobility group box-1 and its role in angiogenesis. J. Leukoc. Biol. 95, 563–574 (2014).

24. Reinmuth, N. et al. Impact of Insulin-Like Growth Factor Receptor-I Function on Angiogenesis, Growth, and Metastasis of Colon Cancer. Lab. Investig. 82, 1377–1389 (2002).

25. Vleugel, M. M., Greijer, A. E., Bos, R., van der Wall, E. & van Diest, P. J. c-Jun activation is associated with proliferation and angiogenesis in invasive breast cancer. Hum. Pathol. 37, 668–674 (2006).

26. Jiang, W. et al. The RNA Methyltransferase METTL3 Promotes Endothelial Progenitor Cell Angiogenesis in Mandibular Distraction Osteogenesis via the PI3K/AKT Pathway . Frontiers in Cell and Developmental Biology vol. 9 (2021).

27. Shemirani, B. & Crowe, D. L. Hypoxic induction of HIF-1α and VEGF expression in head and neck squamous cell carcinoma lines is mediated by stress activated protein kinases. Oral Oncol. 38, 251–257 (2002).

28. Zhu, R. et al. Inhibition of the Notch1 pathway induces peripartum cardiomyopathy. J. Cell. Mol. Med. 24, 7907–7914 (2020).

29. Pugh, C. W. & Ratcliffe, P. J. Regulation of angiogenesis by hypoxia: role of the HIF system. Nat. Med. 9, 677–684 (2003).

30. Hirota, K. & Semenza, G. L. Regulation of angiogenesis by hypoxia-inducible factor 1. Crit. Rev. Oncol. Hematol. 59, 15–26 (2006).

31. Wen, Y. et al. Bclaf1 promotes angiogenesis by regulating HIF-1α transcription in hepatocellular carcinoma. Oncogene 38, 1845–1859 (2019).

32. Pérez, M. et al. Mutual regulation between SIAH2 and DYRK2 controls hypoxic and genotoxic signaling pathways. J. Mol. Cell Biol. 4, 316–330 (2012).

33. Wong, C. S. F. et al. Vascular Normalization by Loss of Siah2 Results in Increased Chemotherapeutic Efficacy. Cancer Res. 72, 1694–1704 (2012).

34. Xiaowei, Z. et al. Hypoxia-induced and calpain-dependent cleavage of filamin A regulates the hypoxic response. Proc. Natl. Acad. Sci. 111, 2560–2565 (2014).

35. Yoo, Y.-G., Kong, G. & Lee, M.-O. Metastasis-associated protein 1 enhances stability of hypoxia-inducible factor-1α protein by recruiting histone deacetylase 1. EMBO J. 25, 1231–1241 (2006).

36. Chen, C. et al. The histone deacetylase HDAC1 activates HIF1α/VEGFA signal pathway in colorectal cancer. Gene 754, 144851 (2020).

37. Zhang, L. et al. HDAC1 knockdown inhibits invasion and induces apoptosis in non-small cell lung cancer cells. Biol. Chem. 399, 603–610 (2018).

38. Houlihan, S. L., Lanctot, A. A., Guo, Y. & Feng, Y. Upregulation of neurovascular communication through filamin abrogation promotes ectopic periventricular neurogenesis. Elife 5, e17823 (2016).

39. Wisniewski, L., French, V., Lockwood, N., Valdivia, L. E. & Frankel, P. P130Cas/bcar1 mediates zebrafish caudal vein plexus angiogenesis. Sci. Rep. 10, 15589 (2020).

40. Yang, L. et al. Antitumor effect of endostatin overexpressed in C6 glioma cells is associated with the down-regulation of VEGF. Int J Oncol 38, 465–471 (2011).

41. Oh, S.-H. et al. Insulin-like growth factor binding protein-3 suppresses vascular endothelial growth factor expression and tumor angiogenesis in head and neck squamous cell carcinoma. Cancer Sci. 103, 1259–1266 (2012).

42. Ohno-Matsui, K., Yoshida, T., Uetama, T., Mochizuki, M. & Morita, I. Vascular endothelial growth factor upregulates pigment epithelium-derived factor expression via VEGFR-1 in human retinal pigment epithelial cells. Biochem. Biophys. Res. Commun. 303, 962–967 (2003).

43. Zha, W., Su, M., Huang, M., Cai, J. & Du, Q. Administration of Pigment Epithelium-Derived Factor Inhibits Airway Inflammation and Remodeling in Chronic OVA-Induced Mice via VEGF Suppression. Allergy Asthma Immunol Res 8, 161–169 (2016).

44. Shirasuna, K. et al. Possible action of vasohibin-1 as an inhibitor in the regulation of vascularization of the bovine corpus luteum. REPRODUCTION 143, 491–500 (2012).

45. Naito, H., Kidoya, H., Sato, Y. & Takakura, N. Induction and Expression of Anti-Angiogenic Vasohibins in the Hematopoietic Stem/Progenitor Cell Population. J. Biochem. 145, 653–659 (2009).

46. Evans, I. M. et al. Vascular Endothelial Growth Factor (VEGF) Promotes Assembly of the p130Cas Interactome to Drive Endothelial Chemotactic Signaling and Angiogenesis * . Mol. Cell. Proteomics 16, 168–180 (2017).

47. Barzelay, A. et al. A potential role for islet-1 in post-natal angiogenesis and vasculogenesis. Thromb Haemost 103, 188–197 (2010).

48. Liu, J. et al. Islet-1 Overexpression in Human Mesenchymal Stem Cells Promotes Vascularization Through Monocyte Chemoattractant Protein-3. Stem Cells 32, 1843–1854 (2014).

49. Xiang, Q. et al. ISL1 overexpression enhances the survival of transplanted human mesenchymal stem cells in a murine myocardial infarction model. Stem Cell Res. Ther. 9, 51 (2018).

50. Li, L., Sun, F., Chen, X. & Zhang, M. ISL1 is upregulated in breast cancer and promotes cell proliferation, invasion, and angiogenesis. Onco. Targets. Ther. 11, 781–789 (2018).

51. Xiong, S.-Q. et al. Role of endogenous insulin gene enhancer protein ISL-1 in angiogenesis. Mol. Vis. 22, 1375–1386 (2016).

52. Zeng, H. et al. Orphan nuclear receptor TR3/Nur77 regulates VEGF-A–induced angiogenesis through its transcriptional activity . J. Exp. Med. 203, 719–729 (2006).

53. Xu, L.-X. et al. Death receptor 3 mediates TNFSF15- and TNFα-induced endothelial cell apoptosis. Int. J. Biochem. Cell Biol. 55, 109–118 (2014).

54. Cho, Y.-L. et al. Specific Activation of Insulin-like Growth Factor-1 Receptor by Ginsenoside Rg5 Promotes Angiogenesis and Vasorelaxation *. J. Biol. Chem. 290, 467–477 (2015).

55. Genetos, D. C., Wong, A., Watari, S. & Yellowley, C. E. Hypoxia increases Annexin A2 expression in osteoblastic cells via VEGF and ERK. Bone 47, 1013–1019 (2010).

56. Zhao, S. et al. Vascular endothelial growth factor upregulates expression of annexin A2 in vitro and in a mouse model of ischemic retinopathy. Mol. Vis. 15, 1231–1242 (2009).

57. Sakurai, D. et al. Crucial Role of Inhibitor of DNA Binding/Differentiation in the Vascular Endothelial Growth Factor-Induced Activation and Angiogenic Processes of Human Endothelial Cells. J. Immunol. 173, 5801 LP – 5809 (2004).

58. TAMURA, K., YOSHIE, M., HASHIMOTO, K. & TACHIKAWA, E. Inhibitory effect of insulin-like growth factor-binding protein-7 (IGFBP7) on in vitro angiogenesis of vascular endothelial cells in the rat corpus luteum. J. Reprod. Dev. 60, 447–453 (2014).

59. Sun, T. et al. Insulin-Like Growth Factor Binding Protein-Related Protein 1 Mediates VEGF-Induced Proliferation, Migration and Tube Formation of Retinal Endothelial Cells. Curr. Eye Res. 36, 341–349 (2011).

60. Lu, S.-J. et al. Robust generation of hemangioblastic progenitors from human embryonic stem cells. Regen. Med. 3, 693–704 (2008).

61. Dragoni, S. & Turowski, P. Polarised VEGFA Signalling at Vascular Blood–Neural Barriers. International Journal of Molecular Sciences vol. 19 (2018).

62. Wang, X. et al. YAP/TAZ Orchestrate VEGF Signaling during Developmental Angiogenesis. Dev. Cell 42, 462-478.e7 (2017).

63. Ha, J. M. et al. Vascular leakage caused by loss of Akt1 is associated with impaired mural cell coverage. FEBS Open Bio 9, 801–813 (2019).

64. Liu, L., Tsai, J. C. & Aird, W. C. Egr-1 gene is induced by the systemic administration of the vascular endothelial growth factor and the epidermal growth factor. Blood 96, 1772–1781 (2000).

65. Huang, S. et al. EZH2 Inhibitor GSK126 Suppresses Antitumor Immunity by Driving Production of Myeloid-Derived Suppressor Cells. Cancer Res. 79, 2009–2020 (2019).

66. Monti, M. et al. PKCε activation promotes FGF-2 exocytosis and induces endothelial cell proliferation and sprouting. J. Mol. Cell. Cardiol. 63, 107–117 (2013).

67. Tripathi, S. & Pandey, K. N. Guanylyl cyclase/natriuretic peptide receptor-A signaling antagonizes the vascular endothelial growth factor-stimulated MAPKs and downstream effectors AP-1 and CREB in mouse mesangial cells. Mol. Cell. Biochem. 368, 47–59 (2012).

68. Zisa, D., Shabbir, A., Mastri, M., Suzuki, G. & Lee, T. Intramuscular VEGF repairs the failing heart: role of host-derived growth factors and mobilization of progenitor cells. Am. J. Physiol. Regul. Integr. Comp. Physiol. 297, R1503–R1515 (2009).

69. Zhao-Jun, L. et al. Regulation of Notch1 and Dll4 by Vascular Endothelial Growth Factor in Arterial Endothelial Cells: Implications for Modulating Arteriogenesis and Angiogenesis. Mol. Cell. Biol. 23, 14–25 (2003).

70. Nazish, S. et al. Clinical trial in a dish using iPSCs shows lovastatin improves endothelial dysfunction and cellular cross-talk in LMNA cardiomyopathy. Sci. Transl. Med. 12, eaax9276 (2020).

71. Yetkin-Arik, B. et al. The role of glycolysis and mitochondrial respiration in the formation and functioning of endothelial tip cells during angiogenesis. Sci. Rep. 9, 12608 (2019).

72. Parra-Bonilla, G., Alvarez, D. F., Alexeyev, M., Vasauskas, A. & Stevens, T. Lactate Dehydrogenase A Expression Is Necessary to Sustain Rapid Angiogenesis of Pulmonary Microvascular Endothelium. PLoS One 8, e75984 (2013).

73. Lin, H. et al. Extracellular Lactate Dehydrogenase A Release From Damaged Neurons Drives Central Nervous System Angiogenesis. eBioMedicine 27, 71–85 (2018).

74. Zhang, X. et al. Downregulation of MST4 Underlies a Novel Inhibitory Role of MicroRNA Let-7a in the Progression of Retinoblastoma. Invest. Ophthalmol. Vis. Sci. 61, 28 (2020).

75. Xu, L. et al. PDCD5 interacts with p53 and functions as a positive regulator in the p53 pathway. Apoptosis 17, 1235–1245 (2012).

76. Seung-Hyun, L. et al. Programmed cell death 5 suppresses AKT-mediated cytoprotection of endothelium. Proc. Natl. Acad. Sci. 115, 4672–4677 (2018).

77. Zhao, H. et al. PDCD5 inhibits osteosarcoma cell metastasis via targeting TGF-β1/Smad signaling pathway and is associated with good prognosis. Am. J. Transl. Res. 11, 1116–1128 (2019).